

Article

Probiotic *Limosilactobacillus reuteri* DSM 17938 Changes Foxp3 Deficiency-Induced Dyslipidemia and Chronic Hepatitis in Mice

Erini Nessim Kostandy ¹, Ji Ho Suh ², Xiangjun Tian ³, Beanna Okeugo ¹, Erin Rubin ⁴, Sara Shirai ⁴, Meng Luo ⁵, Christopher M. Taylor ⁵, Kang Ho Kim ², J. Marc Rhoads ^{1,*} and Yuying Liu ^{1,*}

- ¹ Department of Pediatrics, Division of Gastroenterology, McGovern Medical School, The University of Texas Health Science Center at Houston, Houston, TX 77030, USA; erini.kostandy@gmail.com (E.N.K.); beanna.okeugo@uth.tmc.edu (B.O.)
- ² Department of Anesthesiology, Critical Care and Pain Medicine, McGovern Medical School, The University of Texas Health Science Center at Houston, Houston, TX 77030, USA; ji.ho.suh@uth.tmc.edu (J.H.S.); kangho.kim@uth.tmc.edu (K.H.K.)
- ³ Department of Bioinformatics and Computational Biology, The University of Texas MD Anderson Center, Houston, TX 77030, USA; xiangjun.tian@gmail.com
- ⁴ Department of Pathology and Laboratory Medicine, McGovern Medical School, The University of Texas Health Science Center at Houston, Houston, TX 77030, USA; erin.rubin@uth.tmc.edu (E.R.); sara.shirai@uth.tmc.edu (S.S.)
- ⁵ Department of Microbiology, Immunology and Parasitology, Louisiana State University Health Sciences Center, New Orleans, LA 70112, USA; mluo2@lsuhsc.edu (M.L.)
- * Correspondence: j.marc.rhoads@uth.tmc.edu (J.M.R.); yuying.liu@uth.tmc.edu (Y.L.); Tel.: +1-713-500-5663 (J.M.R.); +1-713-500-5747 (Y.L.)

Abstract: The probiotic *Limosilactobacillus reuteri* DSM 17938 produces anti-inflammatory effects in scurfy (SF) mice, a model characterized by immune dysregulation, polyendocrinopathy, enteropathy, and X-linked inheritance (called IPEX syndrome in humans), caused by regulatory T cell (Treg) deficiency and is due to a Foxp3 gene mutation. Considering the pivotal role of lipids in autoimmune inflammatory processes, we investigated alterations in the relative abundance of lipid profiles in SF mice (\pm treatment with DSM 17938) compared to normal WT mice. We also examined the correlation between plasma lipids and gut microbiota and circulating inflammatory markers. We noted a significant upregulation of plasma lipids associated with autoimmune disease in SF mice, many of which were downregulated by DSM 17938. The upregulated lipids in SF mice demonstrated a significant correlation with gut bacteria known to be implicated in the pathogenesis of various autoimmune diseases. Chronic hepatitis in SF livers responded to DSM 17938 treatment with a reduction in hepatic inflammation. Altered gene expression associated with lipid metabolism and the positive correlation between lipids and inflammatory cytokines together suggest that autoimmunity leads to dyslipidemia with impaired fatty acid oxidation in SF mice. Probiotics are presumed to contribute to the reduction of lipids by reducing inflammatory pathways.

Keywords: probiotics; regulatory T cell; autoimmunity; lipid metabolism; microbiota; inflammation; IPEX syndrome; autoimmune disease; scurfy mouse



Citation: Nessim Kostandy, E.; Suh, J.H.; Tian, X.; Okeugo, B.; Rubin, E.; Shirai, S.; Luo, M.; Taylor, C.M.; Kim, K.H.; Rhoads, J.M.; et al. Probiotic *Limosilactobacillus reuteri* DSM 17938 Changes Foxp3 Deficiency-Induced Dyslipidemia and Chronic Hepatitis in Mice. *Nutrients* **2024**, *16*, 511. <https://doi.org/10.3390/nu16040511>

Academic Editor: Hayley A. Scott

Received: 30 December 2023

Revised: 28 January 2024

Accepted: 7 February 2024

Published: 12 February 2024



Copyright: © 2024 by the authors. Licensee MDPI, Basel, Switzerland. This article is an open access article distributed under the terms and conditions of the Creative Commons Attribution (CC BY) license (<https://creativecommons.org/licenses/by/4.0/>).

1. Introduction

Regulatory T (Treg) cells are crucial for maintaining peripheral tolerance and inflammatory T cell suppression [1,2]. The Forkhead Box protein 3 (Foxp3) gene is a master transcription factor involved in Treg cell development, stability, and function [3,4]. In mice, Foxp3 gene mutation results in the scurfy (SF) mouse model, which serves as a unique model for a rapidly fatal disease characterized by immune dysregulation, polyendocrinopathy, enteropathy, and X-linked inheritance (human IPEX syndrome [5–7]). IPEX syndrome is linked to various autoimmune disorders including type I diabetes (T1DM), eczema, thyroid

dysfunction, interstitial pneumonitis, and renal disease [8]. In addition, there have been case reports of autoimmune hepatitis (AIH) in patients with IPEX syndrome [9].

SF mice develop a severe autoimmune phenotype mediated by uncontrolled Th1 and Th2 cells, resulting in multi-organ failure and premature death before four weeks of age [10,11]. The affected organs include the lungs (pneumonitis), skin (severe dermatitis and autoimmune blistering disease), joints (arthritis), kidneys (glomerulonephritis), and reproductive organs [2,12–14]. Additionally, SF mice demonstrate hematologic abnormalities and display phenotypic features like autoimmune systemic lupus erythematosus (SLE), including the presence of anti-nuclear antibodies, anti-double-stranded DNA antibodies, anti-histone antibodies, and anti-Smith antibodies [15]. In addition, they exhibit histological and biochemical features of AIH and autoimmune cholangitis [16,17].

We previously demonstrated dynamic changes in autoimmunity and gut microbial dysbiosis during the lifespan of SF mice. We were able to modify these changes through intragastric administration of probiotic *Limosilactobacillus reuteri* DSM 17938 (DSM 17938), resulting in marked prolongation of lifespans from <1 month to >4 months [18]. DSM 17938, derived from ATCC 55730, was isolated from a Peruvian mother's breast milk by removing two plasmids harboring antibiotic-resistance genes [19]. This modified strain has been shown to be clinically beneficial in newborn conditions such as infantile colic [20–22] and necrotizing enterocolitis (NEC) [23]. In rodents with experimental NEC, immune deficiency, and healthy newborns, this strain has been observed to reset gut microbial dysbiosis, generate beneficial metabolites, and regulate immune responses [18,24–26]. In SF mice, we identified a unique anti-inflammatory pathway which operates through an adenosine/inosine- A_{2A} -dependent mechanism, resulting in a profound reduction of inflammatory T cells [18,27].

The development of autoimmune disorders is influenced by metabolic disturbances, particularly those related to lipid metabolism. These abnormalities of lipid metabolism are notable in both polygenic autoimmune disorders such as T1DM [28] and in monogenic primary autoimmune diseases such as common variable immunodeficiency (CVID) [29]. Lipids are known to play crucial roles in inflammatory processes [30,31]. For example, some polyunsaturated fatty acids have been shown to have anti-inflammatory effects in autoimmune disorders such as SLE and T1DM, while others are pro-inflammatory [32]. In addition, the gut microbiome plays an important role in regulating intestinal lipid metabolism in both human and animal models [33,34]. Gut microbial dysbiosis may contribute to dysregulating lipid metabolism in primary immune deficiency [35,36] and other diseases such as inflammatory bowel disease (IBD), thereby highlighting the importance of this association and its potential benefit as a therapeutic target [33,37].

The changes in circulating lipids and the association of lipids with gut microbiota and systemic inflammation in SF mice have not been investigated. We hypothesized that *Foxp3* deficiency may be associated with the dysregulation of lipid metabolism. We previously demonstrated dynamic gut microbial dysbiosis throughout the first 21 days of life of SF mice. This dysbiosis was beneficially modulated through the intragastric administration of probiotic DSM 17938 to SF mice [18]. Consequently, we hypothesized that DSM 17938 could alter lipid derangements if it is present. In the current study, we examined plasma lipid profiles and hepatic inflammation in SF mice, comparing the changes to normal mice and SF mice treated with DSM 17938. Our aim was to investigate the potential effect of DSM 17938 on these changes. Additionally, we explored correlations between lipids and gut microbes, circulating inflammatory biomarkers, and liver genes involved in lipid metabolism to further understand the probiotic mechanism of action in Treg-deficient autoimmunity.

2. Materials and Methods

Mice. Wild-type (WT) C57BL/6J (000664) male and heterozygous B6.Cg-*Foxp3*^{sf}/J (004088) female mice, 6–8 weeks old, were purchased from the Jackson Laboratory (Bar Harbor, ME) and were allowed to acclimatize for 2 weeks before setting up breeding pairs for generating SF mice (B6.Cg-*Foxp3*^{sf}/Y). Since the *Foxp3* gene is located on the X

chromosome, only males had SF features, with a 25% probability of total offspring from each litter being SF mice. SF mice were collected from at least 3 different cages per experimental group, and only male mice (either SF or WT littermates) were used in this study.

SF mice exhibited scaly skin on their ears, eyes, and tails and had deformed ears beginning on day of life 13, and early deaths were noted around d24–28 of life [18,38]. Male mice were treated with either control medium or the probiotic beginning on d8 of life, prior to clinical recognition, and were analyzed on d21 of life at the weaning date. The mice were housed under a 12 h light/12 h dark cycle and temperatures of 18–23 °C with 40–60% humidity. They had access to food and water ad libitum in a specific-pathogen-free (SPF) animal facility at the University of Texas Health Science Center at Houston (UTHealth). This study was carried out in accordance with the recommendations of the Guide for the Care and Use of Laboratory Animals of the National Institutes of Health (NIH). The Institutional Animal Care and Use Committee (IACUC) of UTHealth approved the study (protocol numbers: AWC-14-056, AWC-17-0045, and AWC-22-0112).

Preparation of DSM 17938 and treatment of mice. DSM 17938, provided by BioGaiA AB (Stockholm, Sweden), was prepared as described previously [39]. Briefly, DSM 17938 was anaerobically cultured in deMan-Rogosa-Sharpe (MRS) medium at 37 °C for 24 h, and then plated in MRS agar at specific serial dilutions and grown anaerobically at 37 °C for 48–72 h. A quantitative analysis of bacteria in culture media was performed by comparing optical density (OD) 600 nm of cultures at known concentrations using a standard curve of bacterial colony-forming units (CFU)/mL grown on MRS agar. Freshly cultured DSM 17938 bacteria were re-suspended in specified volumes of fresh MRS media based on the calculated CFU required for each feeding, prepared daily for mouse feeding.

Newborn mice were fed with DSM 17938 (10^7 CFU/day in 100 μ L) using intragastric administration, daily, starting from day of life 8 (d8) to d21 (SFL, $n = 5$) or compared with SF mice (SFC, $n = 6$) and WT male littermate controls (WTC, $n = 6$) that were fed with an identical volume of fresh MRS media in the absence of DSM 17938. The dosage and chosen administration method were based on documented evidence of the probiotic strain's efficacy. For infantile colic, beneficial effects were observed with oral administration of $\sim 5 \times 10^8$ CFU (5 drops) in sunflower oil to the babies [22,40,41]. In neonatal experimental NEC in rodents, a daily intragastric administration of 10^6 cfu/g. b.w./day beginning on d10 had been established [24,39,42]. In Treg-deficient SF mice, daily intragastric administration of 10^7 cfu/day until d21 reduced the severity [18,25,43]. Mice were euthanized at age d22 to collect blood and cecal/colonic contents. The isolated plasma and cecal contents were stored immediately at -80 °C for further plasma lipid profile and fecal microbiota analysis.

Plasma global lipid profile analysis. Plasma lipid metabolites were processed and assayed using Metabolon Inc. "www.metabolon.com (accessed on 6 February 2024)" [18]. A total of 212 named lipids in plasma were detected using a non-targeted metabolomic analysis platform including ultra-high-performance liquid chromatography/electrospray ionization tandem mass spectrometry (UPLC-MS/MS) and gas chromatography/mass spectrometry (GC/MS). The lipid profile data included fold changes of SFC/WTC (SF vs. Control) and SFL/SFC (SF+ DSM 17938 treatment vs. SF + MRS treatment) and were reported by Metabolon Inc., with $p < 0.05$ indicating a significant difference between the groups using the Welch's two-sample *t*-test.

Stool microbial community analysis. Sequencing and bioinformatics were performed at Louisiana State University Health Sciences Center Microbial Genomics Resource Group "<http://metagenomics.lsuhscc.edu/mgrg> (accessed on 6 February 2024)". The 16S ribosomal DNA hypervariable region V4 was PCR-amplified using primers V4F GTGCCAGCMGC-CGCGGTAA and V4R GGACTACHVGGGTWTCTAAT with Illumina adaptors and molecular barcodes to produce amplicons. Samples were sequenced on an Illumina MiSeq (Illumina, San Diego, CA, USA) using a 500 cycle V2 sequencing kit to produce 2×250 paired end reads. The forward and reverse-read files were processed using the DADA2 [44] and pipelined in QIIME2 [45]. Amplicon sequence variants were taxonomically classified

using the SILVA v138 database [46]. Bacterial alpha and beta diversity metrics, as well as taxonomic community assessments were performed using QIIME2.

Plasma cytokines, alanine aminotransferase (ALT), and aspartate aminotransferase (AST) measurement. Plasma cytokines IFN- γ and IL-4 were assessed using a mouse proinflammatory assay kit from Meso Scale Discovery (MSD), according to the manufacturer's protocol. Plasma ALT and AST levels were measured using a Beckman Coulter AU480 Chemistry Analyzer using the Center for Comparative Medicine, Pathology Diagnostic Laboratory, Baylor College of Medicine, Houston, Texas, data reported as U/L.

Histological evaluation of hepatitis in mouse livers. Liver tissues collected from mice were fixed and processed using the Cellular and Molecular Morphology Core Laboratory at Texas Medical Center Digestive Diseases Center, Houston, Texas, and stained with hematoxylin and eosin (H & E) for histological evaluation. Hepatitis evaluation was performed by two pathologists independently, using the modified hepatic activity index (abbreviated as modified HAI) grading system. We scored periportal or periseptal interface hepatitis (0 to 4), confluent necrosis (0 to 6), focal lytic necrosis, apoptosis, and focal inflammation (0 to 4), portal inflammation (0 to 4), and modified staging (architectural changes, fibrosis, and cirrhosis) (0 to 6) [47].

Genes associated with lipid metabolism analyzed using a quantitative real-time polymerase chain reaction (RT-qPCR). Total RNA was extracted from mouse liver tissues using the RNeasy Mini Kit (QIAGEN), according to the manufacturer's protocol. The total RNA (500 ng) was reverse transcribed using amfiRivert cDNA synthesis Platinum Master Mix (GenDepot). qRT-PCR was performed using amfiSure qGreen Q-PCR Master Mix (GenDepot) on the CFX Opus 384 Real-Time PCR System (BIO-RAD). The peroxisome proliferator-activated receptor (*Ppara* = *Ppara*) and its target genes [48], genes involved in de novo lipogenesis [49] and genes that are involved in lipid and fatty acid uptake [50,51], were evaluated. All qPCR primers are listed in Supplementary Table S1.

Statistical Analysis. We measured the difference in individual lipid metabolites from the testing groups and reported fold changes; the significance of differences was tested using one-way ANOVA. The upregulated and downregulated lipid metabolites were defined as those with 2.0 (up) or 0.5 (down)-fold changes when associated with a *p*-value < 0.05. Integrative analysis of lipid metabolites and gut microbiota: lipid metabolites and plasma cytokine levels were measured by calculating the Spearman's rank correlation coefficient using the matched samples of each group with both lipid metabolites and microbiota data or plasma cytokine data. A heatmap was plotted using the R package heatmap. For gene expression analysis, to compare the groups of SFC, SFL, and WTC, we used a two-way ANOVA with Tukey's multiple comparisons. For histological parameters, to compare the groups of SFC, SFL, and WTC, we used one-way ANOVA with Tukey's multiple comparisons test using GraphPad Prism version 9.4.1 (GraphPad Software, San Diego, CA, USA). Data are represented as means \pm SD. *p* values < 0.05 were considered statistically significant.

3. Results

3.1. Altered Plasma Lipid Profiles in Treg-Deficiency SF Mice

Altogether, 212 lipid metabolites were identified in the plasma of mice. The SFC group exhibited significant dyslipidemia in comparison to the WTC mice, as evidenced by the significant upregulation of 114 (54%) lipid metabolites, with only 9 (4%) lipids showing downregulation. Specifically, there was a notable increase in the levels of 14 phospholipids, 14 inositols, 12 acylcarnitines, 11 polyunsaturated fatty acids (PUFAs), 11 long-chain FAs (LCFAs), 11 mono- or di-acylglycerols, nine lysolipids, six sphingolipids, four FAs involved in branched-chain amino acid metabolism, three medium-chain FAs (MCFAs), and three acylglycines (Figure 1a). Among the individual upregulated lipids in the SFC group compared to the WTC group, monoacylglycerols and diacylglycerols exhibited the highest fold-change increases, exceeding four times the baseline levels in WTC mice (Figure 1b).

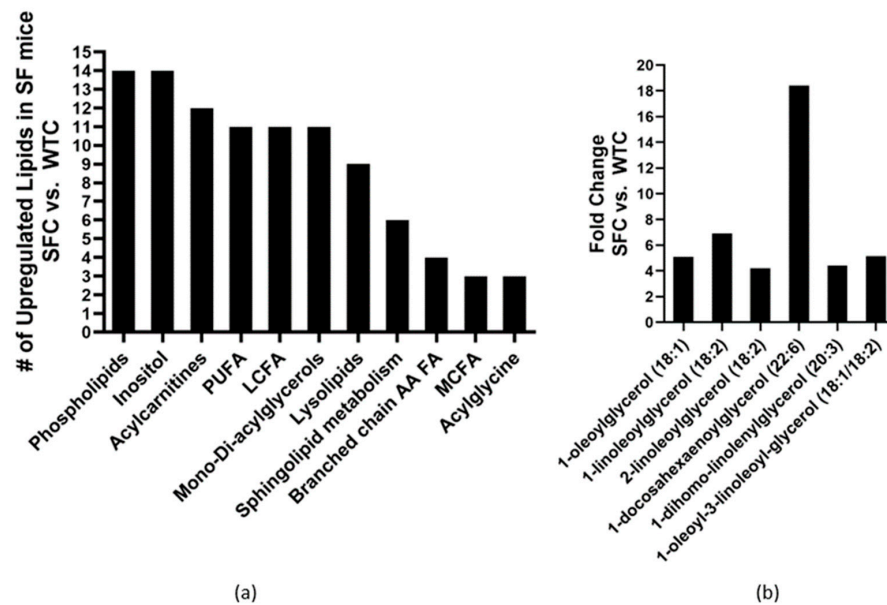


Figure 1. Changed plasma lipid profiles in Treg-deficiency SF mice: (a) the number of lipid sub-pathway categories were upregulated, and (b) Mono- and di-acylglycerols had >4-fold increase in SF mice (SFC, n = 6) compared to WT mice both fed with control media (WTC, n = 6).

3.2. Probiotic DSM 17938 Modulates Plasma Lipid Profile in SF Mice

Intragastric administration of DSM 17938 to SF mice was associated with downregulation of 37 lipids (17%), including sub-pathways phospholipids, acylcarnitine, dihydroxy FA, monoacylglycerol, polyunsaturated FAs, BCAA, and acylglycine. Only four lipids (2%) were upregulated.

Treatment with DSM 17938 resulted in the downregulation of many lipid pathways, including eight phospholipids (the same phospholipids upregulated in SF mice), four acylcarnitines, and MCFAs, three dicarboxylate FAs, and two of each of the following lipid categories, dihydroxy FAs, LCFAs, monoacylglycerol, branched FAs. Additionally, there was downregulation observed in one PUFA and one acylglycine (Figure 2).

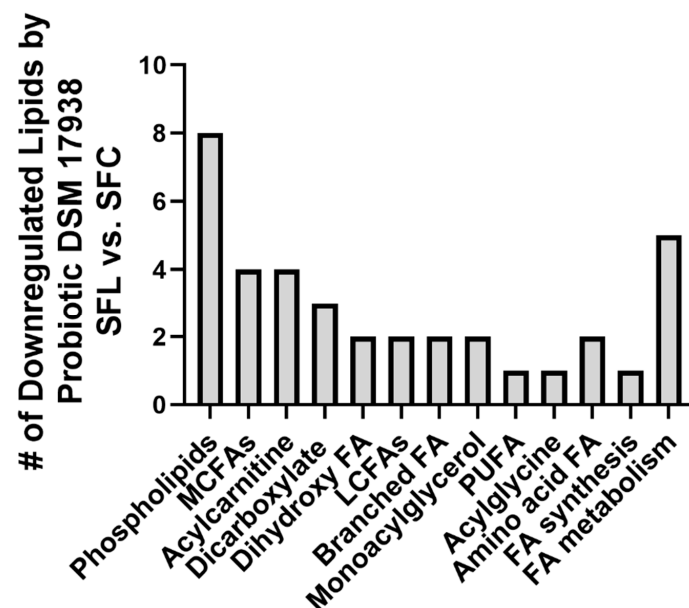


Figure 2. Downregulated plasma lipids in SF mice fed with probiotic DSM 17938. The number of downregulated lipids in SF mice fed with DSM 17938 (SFL, n = 5) was compared to SF mice fed with control media (SFC, n = 6).

3.3. *Foxp3*⁺ Treg Deficiency Reduces Expression of Genes That Are Related to Lipid Metabolism in the Liver of SF Mice

To investigate the mechanism of plasma dyslipidemia caused by Treg-deficiency, we analyzed genes associated with lipid metabolism in the liver of SF mice. PPAR α is a ligand-activated transcription factor that belongs to the steroid hormone receptor superfamily, which is expressed predominantly in tissues that have a high level of fatty acid catabolism [52]. PPAR α regulates the expression of several genes critical for lipid and lipoprotein metabolism [52]. Expression levels of *Ppara* and its targets, as well as genes related to fatty acid synthesis and uptake were downregulated (Figure 3). Notably, intragastric administration of the probiotic did not rescue the inhibition of gene expression levels in SF mice.

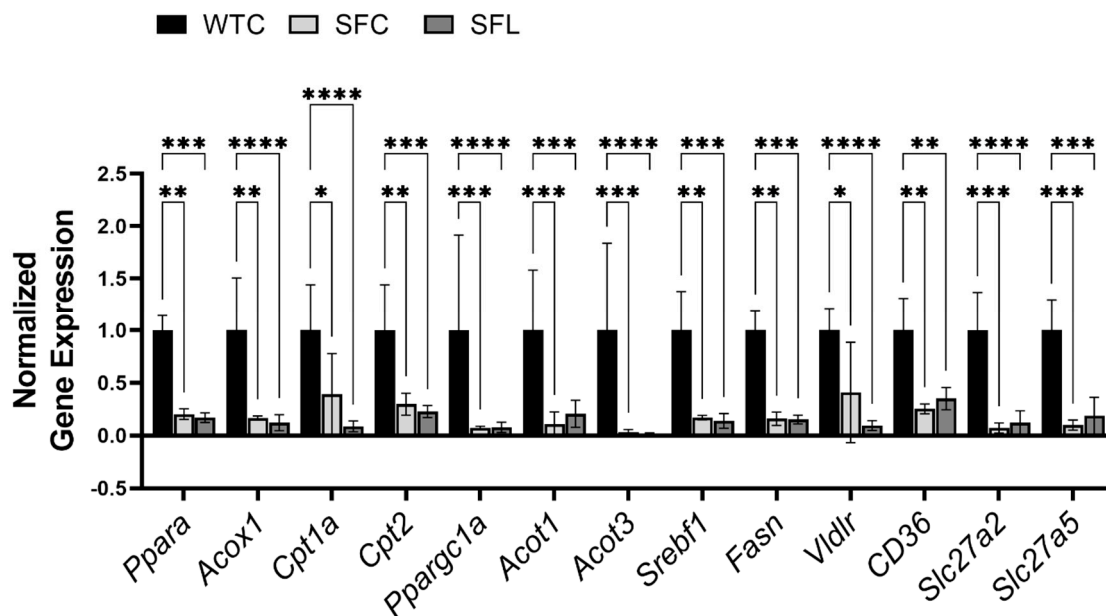


Figure 3. *Foxp3* gene mutation globally and it severely reduced the expression levels of genes that are related to lipid metabolism in the liver of SF mice. *Ppara* and its target genes include acyl-CoA Oxidase 1 (*Acox1*), carnitine palmitoyltransferase (*Cpt1a* and *Cpt2*), peroxisome proliferator-activated receptor gamma coactivator 1-alpha (*Ppargc1a*), and acyl-CoA thioesterase (*Acot1*, and *Acot3*) [48]. Genes involved in de novo lipogenesis [49] include sterol regulatory element binding transcription factor 1 (*Srebf1*) and fatty acid synthase (*Fasn*). Genes involved in lipid and fatty acid uptake [50] include very-low-density lipoprotein receptor (*Vldlr*), FAT atypical cadherin 1 (*CD36 = Fat*), and fatty acid transport proteins *Slc27a2 = Fatp2*, and *Slc27a5 = Fatp5*) [51]. Downregulated genes in SF mice could not be reversed using probiotic treatment. Significant differences between the groups are indicated. WTC n = 6; SFC n = 6; and SFL n = 5. * $p < 0.05$; ** $p < 0.01$; *** $p < 0.001$; **** $p < 0.0001$.

3.4. Altered Plasma Lipids Are Correlated with Gut Microbiota in SF Mice

We have discovered that intragastric administration of DSM 17938 to SF mice ameliorates Treg-associated gut microbial dysbiosis. We found that the decreased Shannon α -diversity associated with Treg deficiency was reversed with DSM 17938 treatment, and that a three-dimensional principal coordinate analysis (PCoA) revealed SF mice with DSM 17938 treatment displayed a shift in microbial community, which was distinct from either WT or SF populations [18,25]. An integrative analysis of changed plasma lipids and gut microbiota revealed a number of correlated alterations, as demonstrated using the HeatMap (Figure 4a). We found that altered lipid metabolites in 19 lipid subpathways significantly correlated with 12 genera of fecal bacteria (Figure 4b). Phospholipids, acylcarnitines, PUFAs, LCFAs, and acylglycerols were associated with several common genera of bacteria. All the upregulated lipids were positively associated with *Escherichia* and were

negatively associated with *Ruminococcus*. Among them, phospholipids correlated with the highest number of bacteria, including seven different bacterial genera. There were 47 acylcarnitine–derivatives correlated with bacteria, showing positive correlation with *Bacteroides*, *Pseudomonas*, *Anaerotruncus*, and *Escherichia*, and negative correlation with *Ruminococcus*, *Anaeroplasma*, *Turicibacter*, and *Akkermansia*. As mentioned, 17 percent of plasma lipids were downregulated by DSM 17938, and these lipids correlated with *Escherichia*, *Pseudomonas*, and *Bacteroides*.

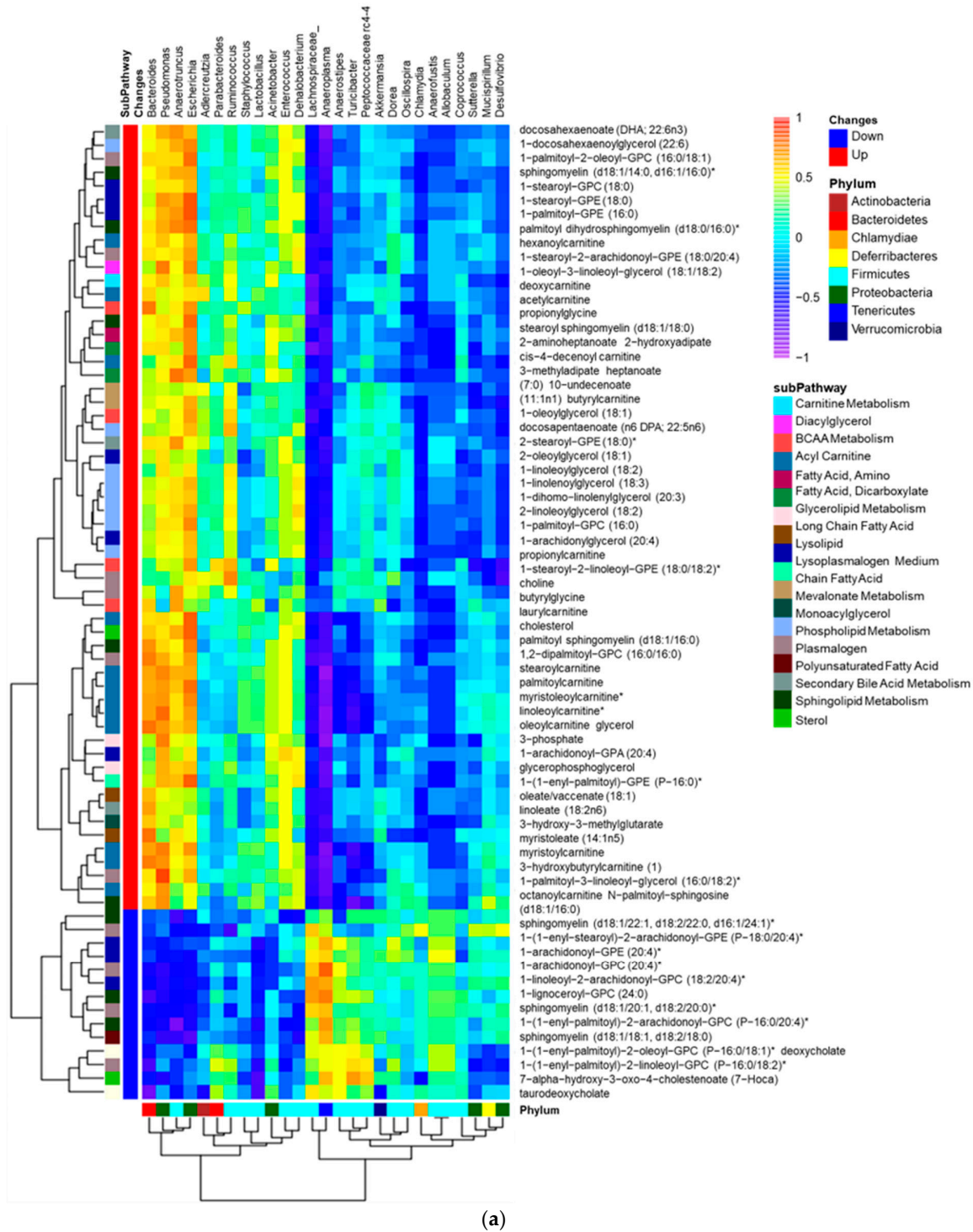


Figure 4. Cont.

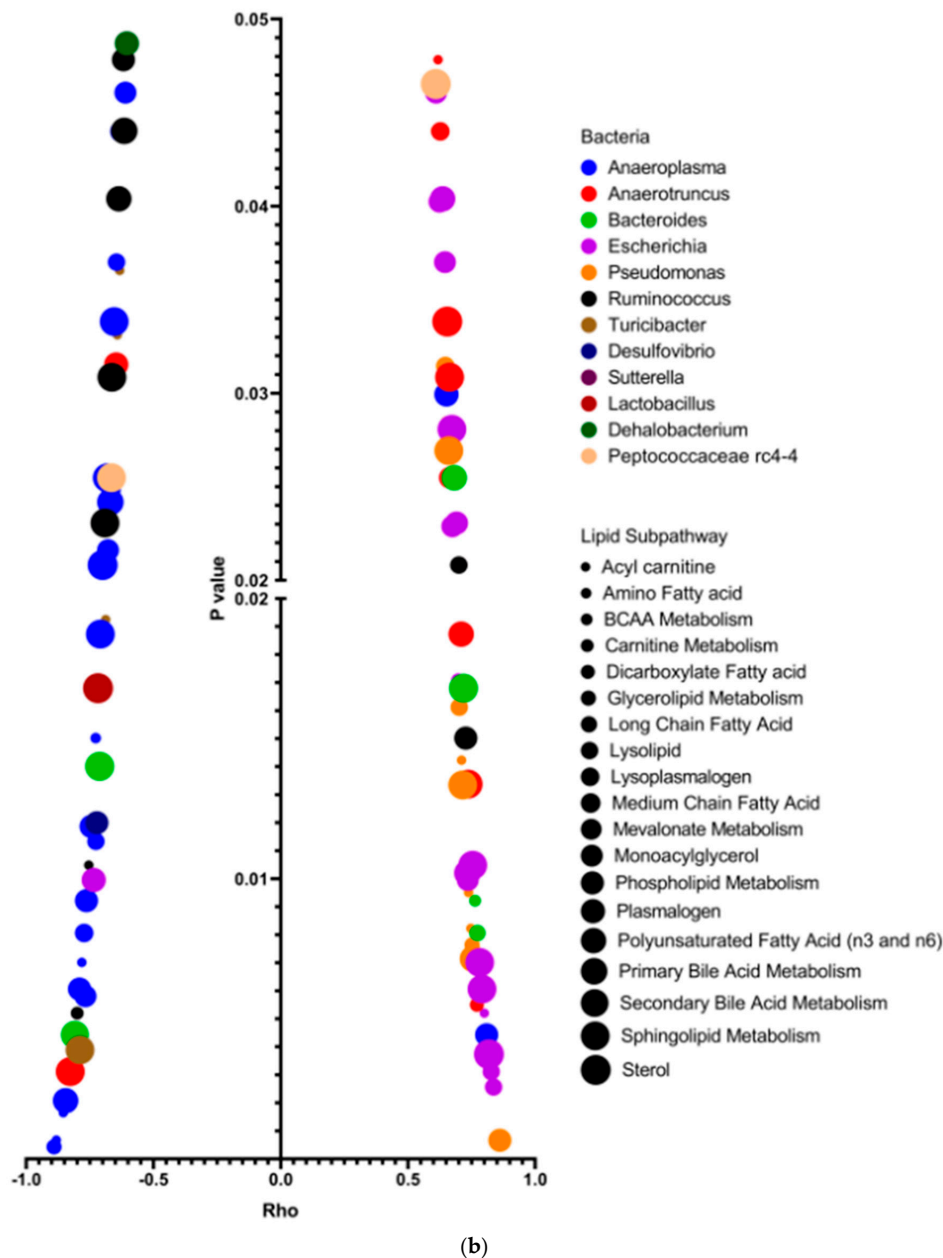


Figure 4. Correlation of gut microbiota and plasma lipids comparing SFC with WTC. (a) Correlation heatmap: bacterial genera (Labeled panel on the top) and lipid metabolites (labeled panel on the right), showing positive (orange/yellow) and negative (blue) correlations with changed lipids in SFC (n = 6) compared to WTC (n = 6). Upregulated (red) lipids and downregulated (blue) lipids are shown; note that most upregulated lipids in SF mice were positively correlated with *Pseudomonas*, *Anaerotruncus*, *Escherichia*, and *Bacteroides*. * indicates compounds that Metabolon Inc. has confident in its identify, however, compounds have not been officially confirmed based on a standard. (b) Dot graph indicating Spearman correlation coefficient Rho (x-axis) and significant correlation p value (<0.05, y-axis) between genera microbiota (the colors) and plasma lipid sub-pathways (the dot sizes) changed in SF mice compared to WT mice. Pearman’s Rho measures the strength of positive (the right) or negative (the left) association between genera microbiota and sub-pathways of lipids. Colors represent different genera of bacteria. Dot sizes represent different lipid sub-pathways. Twelve identified genera were significantly associated with 19 different lipid sub-pathways. Importantly, *Escherichia* (purple), *Pseudomonas* (orange), and *Anaerotruncus* (red) positively correlated significantly with altered levels of lipids, while *Anaeroplasm* (blue) and *Ruminococcus* (black) negatively correlated significantly with altered lipids in SF mice.

3.5. Changed Plasma Lipids Are Positively Correlated with Plasma Th1-Associated (IFN- γ) and Th2-Associated (IL-4) Cytokine Levels

We have previously demonstrated significant increases in plasma Th1- and Th2-associated cytokines in SF mice, levels of which were reduced through intragastric administration of DSM 17938 [18]. Certain lipids have been identified as potential contributors to systemic inflammation in primary autoimmune diseases [29]. To understand which lipid metabolites were associated with Th1- and Th2-associated inflammation, we conducted a correlation analysis between upregulated lipid metabolites and plasma IFN- γ and IL-4. The results showed significant positive correlations between 1-linoleoyl-GPA, caprylate, stearoyl sphingomyelin, taurochenodeoxycholate, and aurohydoxycholic acid with IFN- γ (Table 1). Additionally, three lysolipids, 1-palmitoyl-2-oleoyl-GPC, LCFAs (eicosenoate and erucate), PUFA (adrenate), and 1-(1-enyl-palmitoyl)-GPE were positively correlated with IL-4 (Table 2).

Table 1. Lipid biochemicals associated with IFN- γ in SF mice.

Lipid Pathway	Lipid Biochemical	R Value	p Value
Lysolipid	1-linoleoyl-GPA (18:2)	0.94	0.015
Medium-Chain Fatty Acid	caprylate (8:0)	0.89	0.033
Sphingolipid metabolism	stearoyl sphingomyelin (d18:1/18:0)	0.89	0.033
Primary Bile Acid Metabolism	taurochenodeoxycholate	0.94	0.017
Secondary Bile Acid Metabolism	taurohydoxycholic acid	0.93	0.007

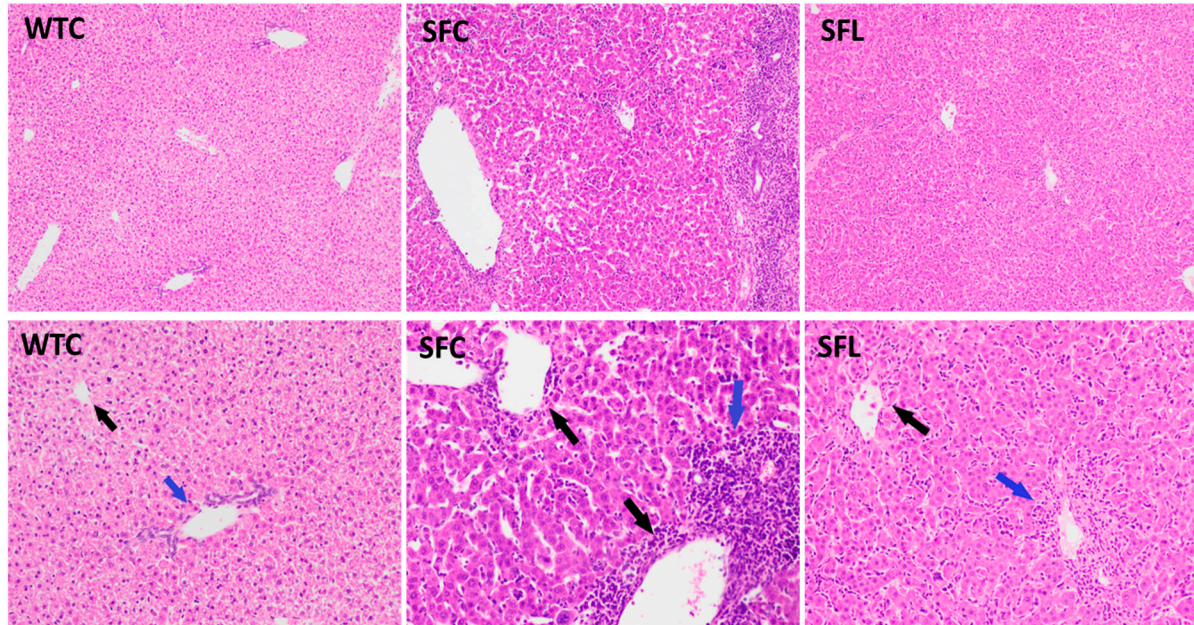
Table 2. Lipid biochemicals associated with IL-4 in SF mice.

Lipid Pathway	Lipid Biochemical	R Value	p Value
Lysolipid	1-(1-enyl-oleoyl)-GPE (P-18:1)	0.94	0.017
	1-stearoyl-GPE (18:0)	0.89	0.033
	1-arachidonoyl-GPA (20:4)	0.99	0.0003
Phospholipid Metabolism	1-palmitoyl-2-oleoyl-GPC (16:0/18:1)	0.89	0.033
Long-Chain Fatty Acid	eicosenoate (20:1)	0.94	0.017
	erucate (22:1n9)	0.94	0.017
Polyunsaturated Fatty Acid	adrenate (22:4n6)	0.94	0.017
Lysoplasmalogen	1-(1-enyl-palmitoyl)-GPE (P-16:0)	0.94	0.017

3.6. *Foxp3*⁺*Treg* Deficiency Induces Chronic Hepatitis and Can Be Partially Reduced through Intragastric Administration of DSM 17938

Although SF mice had significantly upregulated lipids in plasma, hepatic steatosis was not observed in histological evaluation. Instead, the livers of SF mice demonstrated heavy portal tract and periportal chronic inflammation with interface hepatitis, and central and portal vein endothelialitis. With intragastric administration of DSM 17938, SF mice showed marked reduction of the portal tract and subendothelial central vein lymphocytic inflammation (Figure 5a). The average total modified HAI score for SF mice was 5.45 ± 1.48 (of a maximal total score of 24), whereas normal WT mice scored 0 (no changes associated with autoimmunity) (Figure 5b). SF mice scored a mean of 1.95 ± 0.76 in periportal or periseptal interface hepatitis (Figure 5c); 0 in confluent necrosis; 1.25 ± 0.42 in focal lytic necrosis, apoptosis, and focal inflammation (Figure 5d); 2.25 ± 0.67 in portal inflammation (Figure 5e); and 0 in modified staging (no observed architectural changes, fibrosis, or cirrhosis). Interestingly, venous endothelial inflammation involving most of the portal and hepatic venules was much like that seen in AIH and acute T-cell mediated rejection of the liver in human patients. DSM 17938 impacted the total score, periportal or periseptal

interface hepatitis, and portal inflammation scores (Figure 5b,c,e), while no improvement was noted in the focal inflammation score (Figure 5d). However, elevated plasma levels of ALT and AST were not observed in SF mice compared to WT mice (Supplementary Figure S1).



(a)

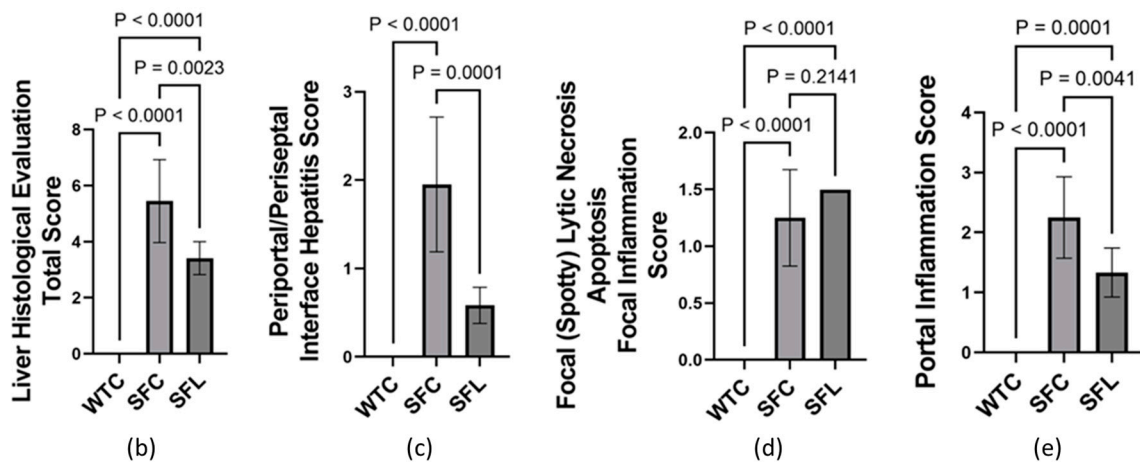


Figure 5. Hepatitis histological evaluation using the modified hepatic activity index (modified HAI) grading system. (a) Photomicrographs of hepatic tissue H&E-stained sections in WTC (left), SFC (middle), and SFL (right). The top panel shows 100× magnification, while the bottom panel shows 200× magnification. Compared to WT mice, SFC mice livers showed heavy portal tract and periportal chronic inflammation with interface hepatitis (blue arrow) and central and portal vein endotheliitis (black arrows). SFL mice with marked reduction of portal tract (blue arrow) and subendothelial central vein lymphocytic inflammation (black arrow). (b) Total histological score = periportal or periseptal interface hepatitis + confluent necrosis + focal inflammation + portal inflammation + architectural changes/fibrosis/cirrhosis. (c) Periportal/periseptal interface hepatitis score. (d) Focal lytic necrosis/apoptosis/focal inflammation. (e) Portal inflammation score. WTC (n = 6), SFC (n = 6), and SFL (n = 5); significant *p* values are indicated in the figures.

4. Discussion

We have uncovered the presence of dyslipidemia in Treg-deficiency-induced autoimmunity. Altered plasma lipids were significantly correlated with systemic inflammation and with specific genera of gut bacteria. Treg-deficiency due to *Foxp3* gene mutation resulted in the histological features of hepatitis which could be ameliorated using gavage feeding DSM 17938. Our study highlights the interplay of liver gene expression, immune cell cytokines, gut microbes, and microbe-associated metabolites in this autoimmune disease.

4.1. Altered Lipid Metabolites in Mice and Humans with Treg-Deficiency Are Associated with Inflammation

Bioactive lipid metabolites play crucial roles in inflammatory processes and regulate immune responses while influencing leukocyte trafficking and clearance in autoimmune diseases [30,53]. Our observations show significant lipid derangements in SF mice, with a >50% elevation of identified lipid metabolites including PUFAs, acylcarnitines, acylglycines (acylglycerols), monoacylglycerol compounds, sphingolipids, and LCFAs. Upregulated lipids are also found in patients with autoimmune conditions such as T1DM, rheumatoid arthritis (RA), multiple sclerosis (MS), SLE, and IBD [54]. In human IPEX syndrome, endocrinopathy evolves during the first year, while T1DM usually develops in the first month of life due to extreme autoimmunological reactions from activated T cells [55]. However, there have been no studies of lipidomics in human IPEX syndrome or in SF mice. In our previous studies, we showed a dynamic progression of autoimmunity development over the first 22d of life. We demonstrated increased levels of IFN- γ and IL-4 in the plasma along with IFN- γ - and IL-4- producing CD4⁺T cells in the spleen. High cytokines were detectable as early as d8 of age, even before the manifestation of clinical symptoms. Notably, these elevated levels of Th1- and Th2-associated cytokines persisted throughout d22 of age [18]. In the current study, we found that the upregulation of lipids positively correlated with circulating IFN- γ and IL-4 levels.

4.2. Categories of Lipids That Are Increased in Autoimmune Diseases

High serum PUFAs, including ω -3 and ω -6, are observed in SLE and correlate with elevated anti-nuclear antibody (ANA) titers, and levels responded to immunosuppressants [56]. Notably, our SF mice also displayed significant elevations in the same PUFAs seen in human SLE, including docosahexaenoic (DHA), eicosapentaenoic acid (EPA), stearidonic, linolenic, and arachidonic acid. Some studies have demonstrated that ω -3 PUFAs have anti-inflammatory functions and could have therapeutic potential in autoimmune diseases [57]. Therefore, it is plausible to hypothesize that the increased PUFAs in SF mice may represent a response to inflammation.

Acylcarnitines, involved in LCFA transportation into the mitochondria, are increased in several autoimmune diseases, and have been used as important diagnostic markers for inborn errors of fatty acid oxidation, as well as markers for energy metabolism, deficits in mitochondrial and peroxisomal β -oxidation activity, insulin resistance and physical activity [58]. Recently they have been identified as potential biomarkers for the diagnosis of SLE [59]. Given the presence of similarities between SF mice and SLE [15], we may postulate that acylcarnitines may also be useful biomarkers in Treg-associated autoimmune disorders [35].

Monoacylglycerol compounds were significantly upregulated in the plasma of patients with systemic sclerosis (SSc). These may function as endogenous cannabinoid ligands involved in SSc pathogenesis [60]. The elevation of sphingolipids, including ceramide, described in SLE and RA, can lead to apoptosis, endothelial dysfunction, and perpetuation of autoimmunity [61]; hence, a similar mechanism may be postulated in Treg-associated autoimmune pathogenesis. It is noteworthy that a diet rich in LCFAs can contribute to nonalcoholic steatohepatitis development in human and guinea pig models [62]. Despite elevated LCFAs in SF mice, liver histology did not show signs of steatosis, indicating that

LCFAs may contribute to hepatitis by exaggerating T helper immune responses rather than causing steatohepatitis.

LCFAs, particularly, very-long-chain fatty acids (VLCFAs), which are abundant in myelin, have been implicated in autoimmune-mediated neuroinflammation, including the development of MS, with evidence of elevated sphingosine-1-phosphate (S1P) levels in glia. Therapeutic effects of S1P inhibition in a mouse model of MS has been reported [63]. Interestingly, it has been previously shown that DSM 17938 reduced the severity of autoimmune encephalomyelitis in a mouse model with MS [64].

4.3. Potential Role of PPAR α in Dyslipidemia and Chronic Hepatitis in SF Mice

The reduced expression levels of genes associated with de novo lipogenesis, lipid and fatty acid uptake, and fatty acid oxidation in SF mice, may be secondary to inflammation in SF mice. The PPAR α pathway is primarily expressed in rodent hepatocytes and is responsible for fat metabolism and carbohydrate homeostasis, as well as cell proliferation and differentiation and inflammation. The roles of PPARs and their receptors in chronic diseases such as diabetes, cancer, and atherosclerosis are well established [65]. PPAR α is a key regulator of fatty acid oxidation, and its activation leads to a decrease in lipid levels and elimination of triglyceride from plasma [66]. PPAR α expression was downregulated in SF mice, along with its target genes, which would inhibit fatty acid oxidation and, subsequently, potentially upregulate lipid levels in the plasma [52,67]. Additionally, PPAR α activation represses NF- κ B signaling, resulting in decreased inflammatory cytokine production by different cell types, with reduced tumor necrosis factor-alpha (TNF- α), IL-6, and IL-1 β [68]. PPAR α inhibits activator protein -1 (AP-1)-dependent genes involved in inflammation and tumor progression [69] and suppresses Th17 cells through modulation of IL-6/STAT3/ROR γ t signaling in rat models of autoimmune myocarditis [70]. The reduction in PPAR α activity in SF mice, coupled with dyslipidemia, may, therefore, be contributing to worsening autoimmunity, inflammation, and hepatitis. PPAR α could potentially serve as a molecular target for the treatment of autoimmune diseases.

Finally, gut bacteria and microbial-associated metabolites, such as bioactive lipids and endocannabinoids could serve as a PPAR α agonist with potential benefits in human diseases [37]. For instance, *Akkermensia muciniphila* can activate PPAR α via modulating endocannabinoid-related lipids, specifically, mono-palmitoyl-glycerols [71]. We, therefore, postulate that changes in the SF mice microbiome, including down regulation of *Akkermensia* species, might be associated with PPAR α downregulation. However, further studies are necessary to validate this hypothesis.

4.4. Potential Clinical Relevance of SF Mouse Chronic Hepatitis Phenotype

Dysfunction or deficiency of Tregs has been linked to the onset and progression of AIH [72]. AIH-associated autoantibodies have been described in patients with IPEX syndrome [9,73]. A recent study reported the clinical, serological, and immunopathological characteristics of AIH with primary biliary cholangitis (PBC) in SF mice [17]. Additionally, central perivenulitis (CP) was observed in SF mice livers, shedding light on the potential use of SF mice as an acute T-cell mediated rejection model in a transplant setting or pharmacologic therapy for human patients with AIH. Indeed, the pathophysiology of SF mice is mainly mediated by Th1 and Th2 cells and their associated cytokines [10,18,74].

4.5. DSM 17938 Impacts Inflammation and Autoimmune-Associated Lipids through Modulating Gut Microbiota and Microbial-Associated Metabolites in SF Mice

Gastrointestinal microbiota dysbiosis can contribute to autoimmune disorders [35,75,76]. Probiotics not only reshape the host microbiota but also impact global metabolic functions, offering potential autoimmune disorder treatments [77]. The gut microbiota influenced by DSM 17938 in SF mice has been associated with metabolic and immunomodulatory regulation [78]. The immunomodulatory mechanisms of DSM 17938 include promoting the maturation of tolerogenic dendritic cells (DCs) via a toll-like receptor (TLR2) and

educating naïve T cell differentiation toward Treg cells [24]. Additionally, DSM 17938 directly inhibits inflammatory effector T cells [42] and inhibits the NF- κ B pathway [39] reducing inflammatory cytokine production during inflammation. Probiotic-educated Treg cells maintain a regulatory function in neonatal stress conditions [79]. The primary mechanism through which Treg cells control inflammatory T cells is through the production of adenosine, which interacts with the adenosine receptor, specifically, A_{2A}. This receptor is predominately present on inflammatory T cells and inhibits their differentiation [80].

In SF mice, the absence of this control mechanism could be reversed by probiotic-derived adenosine and the adenosine metabolite inosine. Adenosine and inosine act as agonists of the adenosine receptor A_{2A} to control inflammation [18,27,43]. DSM 17938 may influence other bacteria-associated metabolites, including amino acids and their derivatives such as glutamine, tryptophan/indoles, and polyamines. These metabolites can regulate the PPAR gamma (PPAR γ) pathway (for example, glutamine), promote Treg cell activation (for example tryptophan-derived indoles), and facilitate renewal of the intestinal mucosa (for example, glutamine and polyamines) [26,81].

We found that DSM 17938 significantly alleviated hepatitis histology in SF mice. However, it only downregulated 17% of lipids, and could not rescue the downregulated genes associated with lipid metabolism. In SF mice, *Pseudomonads*, *Escherichia*, and *Bacteroides* positively correlated with upregulated lipids. These lipids were downregulated by DSM 17938. It is worth noting that the relative abundance (RA) of *Bacteroides* at the genus level in SF mice increased to 30%, which could be reduced to the normal levels of 15% by DSM 17938 [18]. *Bacteroides*, specifically *Bacteroides fragilis* containing the ubiquitin B (UBB) gene, may trigger autoimmune responses due to molecular mimicry in T1DM, IBD, and MS [82]. *P. aeruginosa*, a strain belonging to *Pseudomonads* can cause diseases across diverse host organisms [83].

Conversely, we found that the bacteria *Anaeroplasma* and *Ruminococcus* were negatively correlated with altered lipids in SF mice. These bacteria are generally considered beneficial to protect against autoimmunity. *Anaeroplasma* is stimulated by probiotic *Lactobacillus rhamnosus* GG in rodent models and may have the potential to produce anti-tumor effects [84]. In the setting of a high-fat diet, *Anaeroplasma* may contribute with other commensals to reduce the formation of atherosclerotic plaque [85]. Downregulation of *Ruminococcus* has been also associated with other autoimmune diseases [86]. SF mice showed a marginal reduction in *Ruminococcus* compared to WT mice, while intragastric administration of DSM 17938 to SF mice resulted in recovery of *Ruminococcus* to a level similar level to that in WT mice [18].

Finally, probiotics and gut commensals may cooperate in regulating enterocyte lipid metabolism. For example, L-lactate secreted from *Lactobacillus paracasei* promotes lipid storage, while acetate secreted from *Escherichia coli* stimulates lipid oxidation and consumption in enterocytes [34]. Therefore, exploring the dysfunction of lipid metabolism in SF mice's enterocytes and gut microbial modulation of these processes holds promise for identifying therapeutic targets in these disorders.

4.6. Study Limitations

Our data were analyzed on the weaning day (d22) of SF mice. The illness in SF mice leads to malnutrition because they consume less of the dam's breast milk compared to their WT littermates, and malnutrition may also be a factor affecting the lipid metabolic profile. Also, in human AIH, serum enzyme ALT and AST levels are markedly increased [87]. However, we chose to study mice at less than 1 month of life because of severe multiorgan (including pulmonary) failure, ensuring their survival at the time of testing. These mice were on breast milk, as we intentionally avoided the effects of solid food on gut microbiota in this study. Therefore, we did not analyze liver injury beyond d22 of age. Liver cell death was relatively mild, even though we found lymphocytic infiltration in the face of normal plasma ALT and AST levels.

5. Conclusions

Treg deficiency not only leads to systemic inflammation and malnutrition, but also results in a global increase in plasma lipids with decreased expression of hepatic genes associated with lipid transport, fatty acid oxidation, and de novo lipogenesis. Certain microbial taxa were linked to abnormal lipids, and these lipids were tightly associated with plasma IFN- γ and IL-4 levels. We found that administration of a single probiotic, *L. reuteri* DSM 17938, correlated with shifts in microbial taxa known to improve gut microbial carbohydrate and fat metabolism. *L. reuteri* improved liver periportal infiltration and endotheliitis. Further research on lipid metabolism and its connection with bacterial communities in SF mice may provide diagnostic biomarkers and therapeutic targets for treating autoimmune or transplant-associated liver disease.

Supplementary Materials: The following supporting information can be downloaded at <https://www.mdpi.com/article/10.3390/nu16040511/s1>.

Author Contributions: Conceptualization, Y.L., J.M.R. and K.H.K.; methodology, E.N.K., J.H.S., B.O., E.R., S.S., M.L., C.M.T. and Y.L.; formal analysis, E.N.K., J.H.S., X.T., C.M.T. and Y.L.; writing—original draft preparation, E.N.K.; writing—review and editing, Y.L., J.M.R., K.H.K., E.R., X.T. and C.M.T.; supervision, J.M.R. and Y.L.; funding acquisition, J.M.R., Y.L. and K.H.K. All authors have read and agreed to the published version of the manuscript.

Funding: This study was supported by the National Institutes of Health (NIH)/National Center for Complementary and Integrative Health (NCCIH) Grant R01-AT007083 (to J.M.R. and Y.L.), NIH/National Institute of Allergy and Infectious Diseases (NIAID) Grant R03-AI117442 (to Y.L.), NIH/National Institute of Diabetes and Digestive and Kidney Diseases (NIDDK) Grant R01-DK126656 (to K.H.K.), and, in part, by NIH/NIDDK Grant P30DK056338 of the Texas Medical Center Digestive Diseases Center (to J.M.R.), and Department of Pediatrics, McGovern Medical School, the University of Texas Health Science Center at Houston (to Y.L.).

Institutional Review Board Statement: This study was undertaken in accordance with the recommendation of the Guide for the Care and Use of Laboratory Animal of National Institutes of Health, and the Institutional Animal Care and Use Committee (IACUC) of the University of Texas Health Science Center at Houston approved the protocol (protocol numbers: AWC-14-056, 17-0045 and 22-0112).

Informed Consent Statement: Not applicable.

Data Availability Statement: Most data generated or analyzed during this study are included in this published article. Those data generated and/or analyzed during the current study that are not published here are available from corresponding authors on reasonable request.

Acknowledgments: The probiotic DSM 17938 was obtained as a gift from BioGaia AB (Sweden). We acknowledge the support of BioGaia AB in another research project, but this project was not supported financially by BioGaia AB.

Conflicts of Interest: The authors declare no conflict of interest.

References

1. Sakaguchi, S.; Mikami, N.; Wing, J.B.; Tanaka, A.; Ichiyama, K.; Ohkura, N. Regulatory T Cells and Human Disease. *Annu. Rev. Immunol.* **2020**, *38*, 541–566. [[CrossRef](#)] [[PubMed](#)]
2. Grover, P.; Goel, P.N.; Greene, M.I. Regulatory T Cells: Regulation of Identity and Function. *Front. Immunol.* **2021**, *12*, 750542. [[CrossRef](#)] [[PubMed](#)]
3. Ono, M. Control of regulatory T-cell differentiation and function by T-cell receptor signalling and Foxp3 transcription factor complexes. *Immunology* **2020**, *160*, 24–37. [[CrossRef](#)] [[PubMed](#)]
4. Piccirillo, C.A. Transcriptional and translational control of Foxp3(+) regulatory T cell functional adaptation to inflammation. *Curr. Opin. Immunol.* **2020**, *67*, 27–35. [[CrossRef](#)] [[PubMed](#)]
5. Wildin, R.S.; Freitas, A. IPEX and FOXP3: Clinical and research perspectives. *J. Autoimmun.* **2005**, *25*, 56–62. [[CrossRef](#)] [[PubMed](#)]
6. Kim, J.M.; Rasmussen, J.P.; Rudensky, A.Y. Regulatory T cells prevent catastrophic autoimmunity throughout the lifespan of mice. *Nat. Immunol.* **2007**, *8*, 191–197. [[CrossRef](#)] [[PubMed](#)]

7. Grover, P.; Goel, P.N.; Piccirillo, C.A.; Greene, M.I. FOXP3 and Tip60 Structural Interactions Relevant to IPEX Development Lead to Potential Therapeutics to Increase FOXP3 Dependent Suppressor T Cell Functions. *Front. Pediatr.* **2021**, *9*, 607292. [[CrossRef](#)] [[PubMed](#)]
8. Bacchetta, R.; Roncarolo, M.G. IPEX syndrome from diagnosis to cure, learning along the way. *J. Allergy Clin. Immunol.* **2023**; *in press*. [[CrossRef](#)]
9. López, S.I.; Ciocca, M.; Oleastro, M.; Cuarterolo, M.L.; Rocca, A.; de Dávila, M.T.; Roy, A.; Fernández, M.C.; Nievas, E.; Bosaleh, A.; et al. Autoimmune hepatitis type 2 in a child with IPEX syndrome. *J. Pediatr. Gastroenterol. Nutr.* **2011**, *53*, 690–693. [[CrossRef](#)]
10. Suscovich, T.J.; Perdue, N.R.; Campbell, D.J. Type-1 immunity drives early lethality in scurfy mice. *Eur. J. Immunol.* **2012**, *42*, 2305–2310. [[CrossRef](#)]
11. Haeberle, S.; Raker, V.; Haub, J.; Kim, Y.O.; Weng, S.Y.; Yilmaz, O.K.; Enk, A.; Steinbrink, K.; Schuppan, D.; Hadaschik, E.N. Regulatory T cell deficient scurfy mice exhibit a Th2/M2-like inflammatory response in the skin. *J. Dermatol. Sci.* **2017**, *87*, 285–291. [[CrossRef](#)]
12. Vicari, E.; Haeberle, S.; Bolduan, V.; Ramcke, T.; Vorobyev, A.; Goletz, S.; Iwata, H.; Ludwig, R.J.; Schmidt, E.; Enk, A.H.; et al. Pathogenic Autoantibody Derived from Regulatory T Cell-Deficient Scurfy Mice Targets Type VII Collagen and Leads to Epidermolysis Bullosa Acquisita-Like Blistering Disease. *J. Invest. Dermatol.* **2022**, *142*, 980–984.e4. [[CrossRef](#)]
13. Sharma, R.; Sharma, P.R.; Kim, Y.C.; Leitinger, N.; Lee, J.K.; Fu, S.M.; Ju, S.T. IL-2-controlled expression of multiple T cell trafficking genes and Th2 cytokines in the regulatory T cell-deficient scurfy mice: Implication to multiorgan inflammation and control of skin and lung inflammation. *J. Immunol.* **2011**, *186*, 1268–1278. [[CrossRef](#)] [[PubMed](#)]
14. Ramsdell, F.; Ziegler, S.F. FOXP3 and scurfy: How it all began. *Nat. Rev. Immunol.* **2014**, *14*, 343–349. [[CrossRef](#)] [[PubMed](#)]
15. Hadaschik, E.N.; Wei, X.; Leiss, H.; Heckmann, B.; Niederreiter, B.; Steiner, G.; Ulrich, W.; Enk, A.H.; Smolen, J.S.; Stummvoll, G.H. Regulatory T cell-deficient scurfy mice develop systemic autoimmune features resembling lupus-like disease. *Arthritis Res. Ther.* **2015**, *17*, 35. [[CrossRef](#)] [[PubMed](#)]
16. Zhang, W.; Sharma, R.; Ju, S.T.; He, X.S.; Tao, Y.; Tsuneyama, K.; Tian, Z.; Lian, Z.X.; Fu, S.M.; Gershwin, M.E. Deficiency in regulatory T cells results in development of antimitochondrial antibodies and autoimmune cholangitis. *Hepatology* **2009**, *49*, 545–552. [[CrossRef](#)] [[PubMed](#)]
17. Yilmaz, K.; Haeberle, S.; Kim, Y.O.; Fritzler, M.J.; Weng, S.Y.; Goepfert, B.; Raker, V.K.; Steinbrink, K.; Schuppan, D.; Enk, A.; et al. Regulatory T-cell deficiency leads to features of autoimmune liver disease overlap syndrome in scurfy mice. *Front. Immunol.* **2023**, *14*, 1253649. [[CrossRef](#)] [[PubMed](#)]
18. He, B.; Hoang, T.K.; Wang, T.; Ferris, M.; Taylor, C.M.; Tian, X.; Luo, M.; Tran, D.Q.; Zhou, J.; Tatevian, N.; et al. Resetting microbiota by *Lactobacillus reuteri* inhibits T reg deficiency-induced autoimmunity via adenosine A2A receptors. *J. Exp. Med.* **2017**, *214*, 107–123. [[CrossRef](#)]
19. Rosander, A.; Connolly, E.; Roos, S. Removal of antibiotic resistance gene-carrying plasmids from *Lactobacillus reuteri* ATCC 55730 and characterization of the resulting daughter strain, *L. reuteri* DSM 17938. *Appl. Environ. Microbiol.* **2008**, *74*, 6032–6040. [[CrossRef](#)]
20. Gutierrez-Castrellon, P.; Indrio, F.; Bolio-Galvis, A.; Jimenez-Gutierrez, C.; Jimenez-Escobar, I.; Lopez-Velazquez, G. Efficacy of *Lactobacillus reuteri* DSM 17938 for infantile colic: Systematic review with network meta-analysis. *Medicine* **2017**, *96*, e9375. [[CrossRef](#)]
21. Savino, F.; Cordisco, L.; Tarasco, V.; Palumeri, E.; Calabrese, R.; Oggero, R.; Roos, S.; Matteuzzi, D. *Lactobacillus reuteri* DSM 17938 in infantile colic: A randomized, double-blind, placebo-controlled trial. *Pediatrics* **2010**, *126*, e526–e533. [[CrossRef](#)] [[PubMed](#)]
22. Wadhwa, A.; Kesavelu, D.; Kumar, K.; Chatterjee, P.; Jog, P.; Gopalan, S.; Paul, R.; Veligandla, K.C.; Mehta, S.; Mane, A.; et al. Role of *Lactobacillus reuteri* DSM 17938 on Crying Time Reduction in Infantile Colic and Its Impact on Maternal Depression: A Real-Life Clinic-Based Study. *Clin Pract.* **2022**, *12*, 37–45. [[CrossRef](#)]
23. Gutiérrez Escárate, C.; Bustos Medina, L.; Caniulao Ríos, K.; Taito Antivil, C.; Gallegos Casanova, Y.; Silva Beltrán, C. Probiotic intervention to prevent necrotizing enterocolitis in extremely preterm infants born before 32 weeks of gestation or with a birth weight of less than 1500 g. *Arch. Argent Pediatr.* **2021**, *119*, 185–191. [[PubMed](#)]
24. Hoang, T.K.; He, B.; Wang, T.; Tran, D.Q.; Rhoads, J.M.; Liu, Y. Protective effect of *Lactobacillus reuteri* DSM 17938 against experimental necrotizing enterocolitis is mediated by Toll-like receptor 2. *Am. J. Physiol.-Gastrointest. Liver Physiol.* **2018**, *315*, G231–G240. [[CrossRef](#)]
25. Liu, Y.; Hoang, T.K.; Taylor, C.M.; Park, E.S.; Freeborn, J.; Luo, M.; Roos, S.; Rhoads, J.M. *Limosilactobacillus reuteri* and *Lactis-eibacillus rhamnosus* GG differentially affect gut microbes and metabolites in mice with Treg deficiency. *Am. J. Physiol. Gastrointest. Liver Physiol.* **2021**, *320*, G969–G981. [[CrossRef](#)]
26. Liu, Y.; Tian, X.; Daniel, R.C.; Okeugo, B.; Armbrister, S.A.; Luo, M.; Taylor, C.M.; Wu, G.; Rhoads, J.M. Impact of probiotic *Limosilactobacillus reuteri* DSM 17938 on amino acid metabolism in the healthy newborn mouse. *Amino Acids* **2022**, *54*, 1383–1401. [[CrossRef](#)] [[PubMed](#)]
27. He, B.; Hoang, T.K.; Tran, D.Q.; Rhoads, J.M.; Liu, Y. Adenosine A2A Receptor Deletion Blocks the Beneficial Effects of *Lactobacillus reuteri* in Regulatory T-Deficient Scurfy Mice. *Front. Immunol.* **2017**, *8*, 1680. [[CrossRef](#)] [[PubMed](#)]
28. Parhofer, K.G. Interaction between Glucose and Lipid Metabolism: More than Diabetic Dyslipidemia. *Diabetes Metab. J.* **2015**, *39*, 353–362. [[CrossRef](#)]

29. Jorgensen, S.F.; Macpherson, M.E.; Skarpenland, T.; Berge, R.K.; Fevang, B.; Halvorsen, B.; Aukrust, P. Disturbed lipid profile in common variable immunodeficiency—A pathogenic loop of inflammation and metabolic disturbances. *Front. Immunol.* **2023**, *14*, 1199727. [[CrossRef](#)]
30. Cas, M.D.; Roda, G.; Li, F.; Secundo, F. Functional Lipids in Autoimmune Inflammatory Diseases. *Int. J. Mol. Sci.* **2020**, *21*, 3074. [[CrossRef](#)]
31. Ko, C.W.; Qu, J.; Black, D.D.; Tso, P. Regulation of intestinal lipid metabolism: Current concepts and relevance to disease. *Nat. Rev. Gastroenterol. Hepatol.* **2020**, *17*, 169–183. [[CrossRef](#)] [[PubMed](#)]
32. Poggioli, R.; Hirani, K.; Jogani, V.G.; Ricordi, C. Modulation of inflammation and immunity by omega-3 fatty acids: A possible role for prevention and to halt disease progression in autoimmune, viral, and age-related disorders. *Eur. Rev. Med. Pharmacol. Sci.* **2023**, *27*, 7380–7400. [[PubMed](#)]
33. Wang, Z.; Koonen, D.; Hofker, M.; Fu, J. Gut microbiome and lipid metabolism: From associations to mechanisms. *Curr. Opin. Lipidol.* **2016**, *27*, 216–224. [[CrossRef](#)] [[PubMed](#)]
34. Brown, E.M.; Clardy, J.; Xavier, R.J. Gut microbiome lipid metabolism and its impact on host physiology. *Cell Host Microbe* **2023**, *31*, 173–186. [[CrossRef](#)] [[PubMed](#)]
35. Liu, Y.; Freeborn, J.; Armbrister, S.A.; Tran, D.Q.; Rhoads, J.M. Treg-associated monogenic autoimmune disorders and gut microbial dysbiosis. *Pediatr. Res.* **2022**, *91*, 35–43. [[CrossRef](#)] [[PubMed](#)]
36. Skarpenland, T.; Macpherson, M.E.; Hov, J.R.; Kong, X.Y.; Bohov, P.; Halvorsen, B.; Fevang, B.; Berge, R.K.; Aukrust, P.; Jørgensen, S.F. Altered Plasma Fatty Acids Associate with Gut Microbial Composition in Common Variable Immunodeficiency. *J. Clin. Immunol.* **2022**, *42*, 146–157. [[CrossRef](#)]
37. de Vos, W.M.; Tilg, H.; Van Hul, M.; Cani, P.D. Gut microbiome and health: Mechanistic insights. *Gut* **2022**, *71*, 1020–1032. [[CrossRef](#)]
38. Liu, Y.; Hoang, T.K.; Wang, T.; He, B.; Tran, D.Q.; Zhou, J.; Tatevian, N.; Rhoads, J.M. Circulating L-selectin expressing-T cell subsets correlate with the severity of Foxp3 deficiency autoimmune disease. *Int. J. Clin. Exp. Pathol.* **2016**, *9*, 899–909.
39. Liu, Y.; Fatheree, N.Y.; Mangalat, N.; Rhoads, J.M. *Lactobacillus reuteri* strains reduce incidence and severity of experimental necrotizing enterocolitis via modulation of TLR4 and NF-kappaB signaling in the intestine. *Am. J. Physiol. Gastrointest. Liver Physiol.* **2012**, *302*, G608–G617. [[CrossRef](#)]
40. Sung, V.; D’Amico, F.; Cabana, M.D.; Chau, K.; Koren, G.; Savino, F.; Szajewska, H.; Deshpande, G.; Dupont, C.; Indrio, F.; et al. *Lactobacillus reuteri* to Treat Infant Colic: A Meta-analysis. *Pediatrics* **2018**, *141*, e20171811. [[CrossRef](#)]
41. Savino, F.; Garro, M.; Montanari, P.; Galliano, I.; Bergallo, M. Crying Time and ROR γ /FOXP3 Expression in *Lactobacillus reuteri* DSM17938-Treated Infants with Colic: A Randomized Trial. *J. Pediatr.* **2018**, *192*, 171–177.e1. [[CrossRef](#)]
42. Liu, Y.; Tran, D.Q.; Fatheree, N.Y.; Marc Rhoads, J. *Lactobacillus reuteri* DSM 17938 differentially modulates effector memory T cells and Foxp3+ regulatory T cells in a mouse model of necrotizing enterocolitis. *Am. J. Physiol. Gastrointest. Liver Physiol.* **2014**, *307*, G177–G186. [[CrossRef](#)]
43. Liu, Y.; Armbrister, S.A.; Okeugo, B.; Mills, T.W.; Daniel, R.C.; Oh, J.H.; van Pijkeren, J.P.; Park, E.S.; Saleh, Z.M.; Lahiri, S.; et al. Probiotic-Derived Ecto-5'-Nucleotidase Produces Anti-Inflammatory Adenosine Metabolites in Treg-Deficient Scurfy Mice. *Probiotics Antimicrob. Proteins* **2023**, *15*, 1001–1013. [[CrossRef](#)] [[PubMed](#)]
44. Callahan, B.J.; McMurdie, P.J.; Rosen, M.J.; Han, A.W.; Johnson, A.J.; Holmes, S.P. DADA2: High-resolution sample inference from Illumina amplicon data. *Nat. Methods* **2016**, *13*, 581–583. [[CrossRef](#)] [[PubMed](#)]
45. Bolyen, E.; Rideout, J.R.; Dillon, M.R.; Bokulich, N.A.; Abnet, C.C.; Al-Ghalith, G.A.; Alexander, H.; Alm, E.J.; Arumugam, M.; Asnicar, F.; et al. Reproducible, interactive, scalable and extensible microbiome data science using QIIME 2. *Nat. Biotechnol.* **2019**, *37*, 852–857. [[CrossRef](#)]
46. Pruesse, E.; Quast, C.; Knittel, K.; Fuchs, B.M.; Ludwig, W.; Peplies, J.; Glockner, F.O. SILVA: A comprehensive online resource for quality checked and aligned ribosomal RNA sequence data compatible with ARB. *Nucleic Acids Res.* **2007**, *35*, 7188–7196. [[CrossRef](#)]
47. Nakaji, M.; Hayashi, Y.; Ninomiya, T.; Yano, Y.; Yoon, S.; Seo, Y.; Nagano, H.; Komori, H.; Hashimoto, K.; Orino, A.; et al. Histological grading and staging in chronic hepatitis: Its practical correlation. *Pathol. Int.* **2002**, *52*, 683–690. [[CrossRef](#)]
48. Bougarne, N.; Weyers, B.; Desmet, S.J.; Deckers, J.; Ray, D.W.; Staels, B.; De Bosscher, K. Molecular Actions of PPAR α in Lipid Metabolism and Inflammation. *Endocr. Rev.* **2018**, *39*, 760–802. [[CrossRef](#)] [[PubMed](#)]
49. Aregger, M.; Lawson, K.A.; Billmann, M.; Costanzo, M.; Tong, A.H.Y.; Chan, K.; Rahman, M.; Brown, K.R.; Ross, C.; Usaj, M.; et al. Systematic mapping of genetic interactions for de novo fatty acid synthesis identifies C12orf49 as a regulator of lipid metabolism. *Nat. Metab.* **2020**, *2*, 499–513. [[CrossRef](#)]
50. Son, N.H.; Basu, D.; Samovski, D.; Pietka, T.A.; Peche, V.S.; Willecke, F.; Fang, X.; Yu, S.Q.; Scerbo, D.; Chang, H.R.; et al. Endothelial cell CD36 optimizes tissue fatty acid uptake. *J. Clin. Investig.* **2018**, *128*, 4329–4342. [[CrossRef](#)]
51. Samovski, D.; Jacome-Sosa, M.; Abumrad, N.A. Fatty Acid Transport and Signaling: Mechanisms and Physiological Implications. *Annu. Rev. Physiol.* **2023**, *85*, 317–337. [[CrossRef](#)]
52. Preidis, G.A.; Kim, K.H.; Moore, D.D. Nutrient-sensing nuclear receptors PPAR α and FXR control liver energy balance. *J. Clin. Investig.* **2017**, *127*, 1193–1201. [[CrossRef](#)] [[PubMed](#)]
53. Leuti, A.; Fazio, D.; Fava, M.; Piccoli, A.; Oddi, S.; Maccarrone, M. Bioactive lipids, inflammation and chronic diseases. *Adv. Drug Deliv. Rev.* **2020**, *159*, 133–169. [[CrossRef](#)] [[PubMed](#)]

54. Fernández-Ochoa, Á.; Brunius, C.; Borrás-Linares, I.; Quirantes-Piné, R.; Cádiz-Gurrea, M.L.; Precisesads Clinical, C.; Alarcón Riquelme, M.E.; Segura-Carretero, A. Metabolic Disturbances in Urinary and Plasma Samples from Seven Different Systemic Autoimmune Diseases Detected by HPLC-ESI-QTOF-MS. *J. Proteome Res.* **2020**, *19*, 3220–3229. [[CrossRef](#)]
55. Ben-Skowronek, I. IPEX Syndrome: Genetics and Treatment Options. *Genes* **2021**, *12*, 323. [[CrossRef](#)] [[PubMed](#)]
56. Gorczyca, D.; Szponar, B.; Paściak, M.; Czajkowska, A.; Szmyrka, M. Serum levels of n-3 and n-6 polyunsaturated fatty acids in patients with systemic lupus erythematosus and their association with disease activity: A pilot study. *Scand. J. Rheumatol.* **2022**, *51*, 230–236. [[CrossRef](#)] [[PubMed](#)]
57. Li, X.; Bi, X.; Wang, S.; Zhang, Z.; Li, F.; Zhao, A.Z. Therapeutic Potential of ω -3 Polyunsaturated Fatty Acids in Human Autoimmune Diseases. *Front. Immunol.* **2019**, *10*, 2241. [[CrossRef](#)] [[PubMed](#)]
58. Dambrova, M.; Makrecka-Kuka, M.; Kuka, J.; Vilskersts, R.; Nordberg, D.; Attwood, M.M.; Smesny, S.; Sen, Z.D.; Guo, A.C.; Oler, E.; et al. Acylcarnitines: Nomenclature, Biomarkers, Therapeutic Potential, Drug Targets, and Clinical Trials. *Pharmacol. Rev.* **2022**, *74*, 506–551. [[CrossRef](#)]
59. Wang, Y.; Guo, F.; Guo, Y.; Lu, Y.; Ji, W.; Lin, L.; Chen, W.; Xu, T.; Kong, D.; Shen, Q.; et al. Untargeted lipidomics reveals specific lipid abnormalities in systemic lupus erythematosus. *Clin. Exp. Rheumatol.* **2022**, *40*, 1011–1018. [[CrossRef](#)]
60. Fernández-Ochoa, Á.; Quirantes-Piné, R.; Borrás-Linares, I.; Gemperline, D.; Alarcón Riquelme, M.E.; Beretta, L.; Segura-Carretero, A. Urinary and plasma metabolite differences detected by HPLC-ESI-QTOF-MS in systemic sclerosis patients. *J. Pharm. Biomed. Anal.* **2019**, *162*, 82–90. [[CrossRef](#)]
61. Alexandropoulou, I.; Grammatikopoulou, M.G.; Gkouskou, K.K.; Pritsa, A.A.; Vassilakou, T.; Rigopoulou, E.; Lindqvist, H.M.; Bogdanos, D.P. Ceramides in Autoimmune Rheumatic Diseases: Existing Evidence and Therapeutic Considerations for Diet as an Anticeramide Treatment. *Nutrients* **2023**, *15*, 229. [[CrossRef](#)]
62. Pedersen, K.; Ipsen, D.H.; Skat-Rørdam, J.; Lykkesfeldt, J.; Tveden-Nyborg, P. Dietary Long-Chain Fatty Acids Accelerate Metabolic Dysfunction in Guinea Pigs with Non-Alcoholic Steatohepatitis. *Nutrients* **2023**, *15*, 2445. [[CrossRef](#)] [[PubMed](#)]
63. Mohammad, N.S.; Nazli, R.; Zafar, H.; Fatima, S. Effects of lipid based Multiple Micronutrients Supplement on the birth outcome of underweight pre-eclamptic women: A randomized clinical trial. *Pak. J. Med. Sci.* **2022**, *38*, 219–226. [[PubMed](#)]
64. He, B.; Hoang, T.K.; Tian, X.; Taylor, C.M.; Blanchard, E.; Luo, M.; Bhattacharjee, M.B.; Freeborn, J.; Park, S.; Couturier, J.; et al. *Lactobacillus reuteri* Reduces the Severity of Experimental Autoimmune Encephalomyelitis in Mice by Modulating Gut Microbiota. *Front. Immunol.* **2019**, *10*, 385. [[CrossRef](#)]
65. Mirza, A.Z.; Althagafi, I.I.; Shamshad, H. Role of PPAR receptor in different diseases and their ligands: Physiological importance and clinical implications. *Eur. J. Med. Chem.* **2019**, *166*, 502–513. [[CrossRef](#)]
66. Tahri-Joutey, M.; Andreoletti, P.; Surapureddi, S.; Nasser, B.; Cherkaoui-Malki, M.; Latruffe, N. Mechanisms Mediating the Regulation of Peroxisomal Fatty Acid Beta-Oxidation by PPAR α . *Int. J. Mol. Sci.* **2021**, *22*, 8969. [[CrossRef](#)] [[PubMed](#)]
67. Stec, D.E.; Gordon, D.M.; Hipp, J.A.; Hong, S.; Mitchell, Z.L.; Franco, N.R.; Robison, J.W.; Anderson, C.D.; Stec, D.F.; Hinds, T.D., Jr. Loss of hepatic PPAR α promotes inflammation and serum hyperlipidemia in diet-induced obesity. *Am. J. Physiol.-Regul. Integr. Comp. Physiol.* **2019**, *317*, R733–R745. [[CrossRef](#)]
68. Decara, J.; Rivera, P.; Lopez-Gambero, A.J.; Serrano, A.; Pavon, F.J.; Baixeras, E.; Rodriguez de Fonseca, F.; Suarez, J. Peroxisome Proliferator-Activated Receptors: Experimental Targeting for the Treatment of Inflammatory Bowel Diseases. *Front. Pharmacol.* **2020**, *11*, 730. [[CrossRef](#)]
69. Grau, R.; Punzón, C.; Fresno, M.; Iñiguez, M.A. Peroxisome-proliferator-activated receptor alpha agonists inhibit cyclo-oxygenase 2 and vascular endothelial growth factor transcriptional activation in human colorectal carcinoma cells via inhibition of activator protein-1. *Biochem. J.* **2006**, *395*, 81–88. [[CrossRef](#)]
70. Chang, H.; Zhao, F.; Xie, X.; Liao, Y.; Song, Y.; Liu, C.; Wu, Y.; Wang, Y.; Liu, D.; Wang, Y.; et al. PPAR α suppresses Th17 cell differentiation through IL-6/STAT3/ROR γ t pathway in experimental autoimmune myocarditis. *Exp. Cell Res.* **2019**, *375*, 22–30. [[CrossRef](#)]
71. Depommier, C.; Vitale, R.M.; Iannotti, F.A.; Silvestri, C.; Flamand, N.; Druart, C.; Everard, A.; Pelicaen, R.; Maiter, D.; Thissen, J.P.; et al. Beneficial Effects of Akkermansia muciniphila Are Not Associated with Major Changes in the Circulating Endocannabinoidome but Linked to Higher Mono-Palmitoyl-Glycerol Levels as New PPAR α Agonists. *Cells* **2021**, *10*, 185. [[CrossRef](#)]
72. Chen, J.; Liu, W.; Zhu, W. Foxp3(+) Treg Cells Are Associated with Pathological Process of Autoimmune Hepatitis by Activating Methylation Modification in Autoimmune Hepatitis Patients. *Med. Sci. Monit.* **2019**, *25*, 6204–6212. [[CrossRef](#)] [[PubMed](#)]
73. Agakidis, C.; Agakidou, E.; Sarafidis, K.; Papoulidis, I.; Xinias, I.; Farmaki, E. Immune Dysregulation, Polyendocrinopathy, Enteropathy, X-Linked Syndrome Associated with a Novel Mutation of FOXP3 Gene. *Front. Pediatr.* **2019**, *7*, 20. [[CrossRef](#)] [[PubMed](#)]
74. Lee, G.; Chung, H.S.; Lee, K.; Lee, H.; Kim, M.; Bae, H. Curcumin attenuates the scurfy-induced immune disorder, a model of IPEX syndrome, with inhibiting Th1/Th2/Th17 responses in mice. *Phytomedicine* **2017**, *33*, 1–6. [[CrossRef](#)] [[PubMed](#)]
75. Belvoncikova, P.; Maronek, M.; Gardlik, R. Gut Dysbiosis and Fecal Microbiota Transplantation in Autoimmune Diseases. *Int. J. Mol. Sci.* **2022**, *23*, 10729. [[CrossRef](#)] [[PubMed](#)]
76. De Luca, F.; Shoenfeld, Y. The microbiome in autoimmune diseases. *Clin. Exp. Immunol.* **2019**, *195*, 74–85. [[CrossRef](#)] [[PubMed](#)]
77. Liu, Y.; Alookaran, J.J.; Rhoads, J.M. Probiotics in Autoimmune and Inflammatory Disorders. *Nutrients* **2018**, *10*, 1537. [[CrossRef](#)] [[PubMed](#)]

78. Liu, Y.; Tran, D.Q.; Rhoads, J.M. Probiotics in Disease Prevention and Treatment. *J. Clin. Pharmacol.* **2018**, *58* (Suppl. 10), S164–S179. [[CrossRef](#)] [[PubMed](#)]
79. Liu, Y.; Hoang, T.K.; Park, E.S.; Freeborn, J.; Okeugo, B.; Tran, D.Q.; Rhoads, J.M. Probiotic-educated Tregs are more potent than naive Tregs for immune tolerance in stressed new-born mice. *Benef. Microbes* **2023**, *14*, 73–84. [[CrossRef](#)]
80. Da, M.; Chen, L.; Enk, A.; Ring, S.; Mahnke, K. The Multifaceted Actions of CD73 During Development and Suppressive Actions of Regulatory T Cells. *Front. Immunol.* **2022**, *13*, 914799. [[CrossRef](#)]
81. Liu, Y.; Tian, X.; He, B.; Hoang, T.K.; Taylor, C.M.; Blanchard, E.; Freeborn, J.; Park, S.; Luo, M.; Couturier, J.; et al. *Lactobacillus reuteri* DSM 17938 feeding of healthy newborn mice regulates immune responses while modulating gut microbiota and boosting beneficial metabolites. *Am. J. Physiol. Gastrointest. Liver Physiol.* **2019**, *317*, G824–G838. [[CrossRef](#)]
82. Zafar, H.; Saier, M.H., Jr. Gut Bacteroides species in health and disease. *Gut Microbes* **2021**, *13*, 1–20. [[CrossRef](#)]
83. Silby, M.W.; Winstanley, C.; Godfrey, S.A.; Levy, S.B.; Jackson, R.W. Pseudomonas genomes: Diverse and adaptable. *FEMS Microbiol. Rev.* **2011**, *35*, 652–680. [[CrossRef](#)]
84. Liu, X.; Jin, G.; Tang, Q.; Huang, S.; Zhang, Y.; Sun, Y.; Liu, T.; Guo, Z.; Yang, C.; Wang, B.; et al. Early life *Lactobacillus rhamnosus* GG colonisation inhibits intestinal tumour formation. *Br. J. Cancer* **2022**, *126*, 1421–1431. [[CrossRef](#)]
85. Chan, Y.K.; Brar, M.S.; Kirjavainen, P.V.; Chen, Y.; Peng, J.; Li, D.; Leung, F.C.; El-Nezami, H. High fat diet induced atherosclerosis is accompanied with low colonic bacterial diversity and altered abundances that correlates with plaque size, plasma A-FABP and cholesterol: A pilot study of high fat diet and its intervention with *Lactobacillus rhamnosus* GG (LGG) or telmisartan in ApoE(-/-) mice. *BMC Microbiol.* **2016**, *16*, 264.
86. Wang, T.; Sternes, P.R.; Guo, X.K.; Zhao, H.; Xu, C.; Xu, H. Autoimmune diseases exhibit shared alterations in the gut microbiota. *Rheumatology* **2023**, Kead364. [[CrossRef](#)] [[PubMed](#)]
87. Suci, A.; Abenavoli, L.; Pellicano, R.; Luzza, F.; Dumitrascu, D.L. Transaminases: Oldies but goldies. A narrative review. *Minerva Gastroenterol. Dietol.* **2020**, *66*, 246–251. [[CrossRef](#)] [[PubMed](#)]

Disclaimer/Publisher’s Note: The statements, opinions and data contained in all publications are solely those of the individual author(s) and contributor(s) and not of MDPI and/or the editor(s). MDPI and/or the editor(s) disclaim responsibility for any injury to people or property resulting from any ideas, methods, instructions or products referred to in the content.